AIAA JOURNAL
Vol. 40, No. 9, September 2002

Temperature Profile Influence on Layered Plates Response Considering Classical and Advanced Theories

Erasmo Carrera*
Politecnico di Torino, 10129 Turin, Italy

A study on the influence of the through-the-thickness temperature profile $T(z)$ on the thermomechanical response of multilayered anisotropic thick and thin plates has been conducted. The heat conduction problem is solved, and the temperature variation $T_c(z)$ is then calculated. The governing thermomechanical equations of multilayered plates are written considering a large variety of classical and advanced or zigzag theories into account. The principle of virtual displacement and the Reissner mixed variational theorem are employed. Linear, up to fourth-order expansions in z are retained for the assumed transverse stress and displacement fields. As a result, more than 20 plate theories are compared. The numerical investigation is restricted to orthotropic layered plates with harmonic in-plane distribution of both thermal loadings and unknown variables. Four sample plate problems are treated that are related to plates made of isotropic and/or orthotropic layers that are loaded by different top–bottom plate surface temperature conditions. Comparison is made to results related to a linear profile $T_a(z)$, which is usually assumed in open literature. The following is concluded: Thick plates could exhibit a layerwise form temperature profile $T_c(z)$. $T_a(z)$ case is approached for thin plate geometries. The use of linear temperature profile leads to large errors in tracing the response of thick plate geometries. The accuracy of plate theories is affected to great extent by the form of temperature variation $T(z)$. Refinements of classical plate theories can be meaningless unless the calculated $T_c(z)$ is introduced. The layerwise form of $T_c(z)$ would require layerwise assumptions for stresses and/or displacements. Plate theories that neglect transverse normal strains lead to very inaccurate results in both thick and thin plates analysis. At least a parabolic expansion for transverse displacement is required to capture transverse normal thermal strains that vary linearly along the plate thickness.

Nomenclature

a, b, h	=	plate geometrical parameters (length, width, and thickness)
k	=	sub/superscript used to denote parameters related to k layer
N	=	order of expansions used for transverse stresses and displacements
N_l	=	number of constituent layers of multilayered plate/shell
$T_a(z)$	=	temperature profile having linear form in the plate thickness equation (1)
$T_c(z)$	=	temperature profile from the solution of heat conduction problem equation (16)
T_e	=	value of environmental temperature
x, y, z	=	Cartesian coordinates reference systems for plates
Γ	=	boundary of Ω
Ω	=	plate reference surface

Introduction

STRESS fields related to temperature variations often represent a contributing factor and, in some cases, are the main causes of the failure of structures. Because of their detrimental implications, the effects of both high-temperature and mechanical loadings have to be considered in the earliest stages of the design process of such structures. Thin-walled members of reactor vessels, turbines, as well as the structures of future supersonic and hypersonic vehicles, such as high-speed civil transport and advanced tactical fighters, are particularly susceptible to failure resulting from excessive stress levels induced by thermal or combined thermomechanical loadings.[1] Thermal deformations also play a fundamental role in multilayered thin-film regions, comprising optical mirrors,[2] as well as in space reflector antennas, which require stringent geometric tolerance compared to traditional structures.[3] The importance of the thermal stress analysis of smart structures has recently been demonstrated in Ref. 4, where a full, coupled thermopiezoelectric–mechanical model was presented. Large sections of the aforementioned structures, such as traditional sandwich panels, panels made of anisotropic composite materials or layered isotropic structures used as thermal protection, are made up of multilayered plate and shell constructions.

The present work is restricted to plate geometries. Early[5,6] and recent[2,7,8] exact three-dimensional solutions have shown that appropriate structural modelings are required to describe what was summarized in Ref. 9 as C_z^0–requirements, that is, to account for zigzag effects and interlaminar continuity, both displacement and transverse stress fields must be C^0–continuous functions in the plate thickness direction z.

Many papers have appeared in which classical and advanced theories have been proposed and applied. Several reviews are available on this topic. Among these are those by Tauchert,[10] Noor and Burton,[11] and Argyris and Tenek,[12] as well as that by Reddy.[13] A discussion on those contributions related to the bending of anisotropic plates has been provided in a recent work of the present author.[14] Readers who are interested may refer to Ref. 14 for an overview and literature. Note a conclusion that has been reached by Murakami[2]: "in order to predict rapid variation of transverse normal strains, a plate theory with cubic variation of in-plane displacement in each layer, rather than over the entire plate thickness, should be adopted. Otherwise full three dimensional analyses are recommended." In other words, due to the intrinsic through-the-thickness variation of thermal loadings, a layerwise description is required to describe accurately the local response of layered plates. The conclusions recently reached by Bhaskar and Varadan,[15] who underlined the importance of refined theories to handle thermal loadings accurately with respect to mechanical ones, are also relevant.

Most of the available literature on the thermomechanical response of multilayered plates, including three-dimensional solutions[8] assumes a temperature profile $T_a(z)$, which varies linearly in the plate thickness direction z, for example,

$$T_a(z) = T_b + [(T_t - T_b)/h]z \tag{1}$$

Received 26 June 2001; revision received 17 January 2002; accepted for publication 30 January 2002.

*Professor of Aerospace Structures and Applied Aeroelasticity, Department of Aeronautics and Aerospace Engineering, Corso Duca degli Abruzzi 24; carrera@polito.it. Member AIAA.

T_t and T_b are the temperature with correspondence to the top and bottom plate surfaces, respectively, and h is the plate thickness. On the other hand, Tungikar and Rao[7] have demonstrated, by solving the heat conduction problems, that thick anisotropic multilayered plates could show a layerwise form of $T_c(z)$. That is, $T_c(z)$ can differ considerably from the linear one in Eq. (1). The importance of including higher-order temperature variation has been recently been demonstrated by Zhou et al.[4] and Gu et al.[16]

In the described scenarios, it could be of interest to contribute to the following topics: 1) evaluating the influence of the temperature profile on the response of multilayered plates, as well as to compare the two cases of thermal loading profiles $T_a(z)$ and $T_c(z)$, and 2) weighing the approximations of a given plate theory with those introduced using an assumed linear temperature profile $T_a(z)$. To address these two topics, it appears mandatory to develop a thermomechanical plate model that permits us to introduce any form of temperature profile (linear, higher-order, as well as layerwise form), as well as to take into account both classical and advanced plate theories.

The aim of the present paper is contributing to the aforementioned. The heat conduction problems are solved, according to the technique presented by Tungikar and Rao.[7] The recent findings of the present author's previous works[17–21] are then extended to include a temperature profile as it originates from the solution of heat conduction problems. As a result, the thermomechanical problem is presented taking a large variety of so-called classical and advanced zigzag theories into account. Classical theories formulated on the bases of the principle of virtual displacements (PVD), with only displacement variables, are compared to refined theories, formulated on the basis of the Reissner mixed variational theorem (RMVT), which introduces an independent transverse stress field (including transverse normal stress σ_{zz} in each plate layer). The layerwise (LW) descriptions,[13] where unknowns are independent in each layer, are compared to the equivalent single layer (ESL) descriptions, where the number of the variables is preserved independent from the number of the constitutive layers. (Linear, up to fourth-order z expansions are considered for both transverse stresses and displacements.) Numerical evaluations are given for four selected problems related to different materials, layouts (isotropic, composites, and sandwich plates), and thermal loadings conditions, as well as geometrical parameters.

Preliminary

The geometry and Cartesian coordinate system x, y, z of the multilayered plates made of N_l layers are shown in Fig. 1. The lamina are considered homogeneous and to operate in the linear elastic range. Stiffness coefficients of Hooke's law for the anisotropic k lamina are employed in standard form. This reads $\sigma_i^k = \tilde{C}_{ij}^k \epsilon_j^k$, where indices i and j, ranging from 1 to 6, stand for the index couples 11, 22, 33, 13, 23, and 12, respectively. The material is assumed to be orthotropic, as specified by Ref. 13: $\tilde{C}_{14} = \tilde{C}_{24} = \tilde{C}_{34} = \tilde{C}_{64} = \tilde{C}_{15} = \tilde{C}_{25} = \tilde{C}_{35} = \tilde{C}_{65} = 0$. This implies that σ_{xz}^k and σ_{yz}^k depend only on ϵ_{xz}^k and ϵ_{yz}^k. In matrix form,

$$\boldsymbol{\sigma}_{pH}^k = \tilde{\boldsymbol{C}}_{pp}^k \boldsymbol{\epsilon}_{pG}^k + \tilde{\boldsymbol{C}}_{pn}^k \boldsymbol{\epsilon}_{nG}^k, \qquad \boldsymbol{\sigma}_{nH}^k = \tilde{\boldsymbol{C}}_{np}^k \boldsymbol{\epsilon}_{pG}^k + \tilde{\boldsymbol{C}}_{nn}^k \boldsymbol{\epsilon}_{nG}^k \quad (2)$$

in which subscripts p and n denote in-plane and out-of-plane (normal) components ($\boldsymbol{\sigma}_p^k = \{\sigma_{xx}^k, \sigma_{yy}^k, \sigma_{xy}^k\}$ and $\boldsymbol{\sigma}_n^k = \{\sigma_{xz}^k, \sigma_{yz}^k, \sigma_{zz}^k\}$) and H and G indicate values from Hooke's law and from geometrical Eq. (6) relations, respectively. Subscript d denotes values related to the standard displacement formulation. Boldface letters are here used for arrays.

Thermal stresses (subscript T) are induced in the k layer by thermal strains according to material behavior as follows:

$$\boldsymbol{\sigma}_{pT_d}^k = \tilde{\boldsymbol{C}}_{pp}^k \boldsymbol{\epsilon}_{pT}^k + \tilde{\boldsymbol{C}}_{pn}^k \boldsymbol{\epsilon}_{nT}^k, \qquad \boldsymbol{\sigma}_{nT_d}^k = \tilde{\boldsymbol{C}}_{np}^k \boldsymbol{\epsilon}_{pT}^k + \tilde{\boldsymbol{C}}_{nn}^k \boldsymbol{\epsilon}_{nT}^k \quad (3)$$

where the strains are related to a given temperature gradient $T^k(x, y, z)$ according to the thermal expansion coefficients α_{ij} of the layer:

$$\boldsymbol{\epsilon}_{pT}^k = \left\{\alpha_{xx}^k, \alpha_{yy}^k, \alpha_{xy}^k\right\} T^k(x, y, z) = \boldsymbol{\alpha}_p^k T^k(x, y, z)$$

$$\boldsymbol{\epsilon}_{nT}^k = \left\{\alpha_{xz}^k, \alpha_{yz}^k, \alpha_{zz}^k\right\} T^k(x, y, z) = \boldsymbol{\alpha}_n^k T^k(x, y, z) \quad (4)$$

For the adopted mixed-solution procedure, the stress–strain relationships are conveniently put in the following mixed form:

$$\boldsymbol{\sigma}_{pH}^k = \boldsymbol{C}_{pp}^k \boldsymbol{\epsilon}_{pG}^k + \boldsymbol{C}_{pn}^k \boldsymbol{\sigma}_{nM}^k, \qquad \boldsymbol{\epsilon}_{nH}^k = \boldsymbol{C}_{np}^k \boldsymbol{\epsilon}_{pG}^k + \boldsymbol{C}_{nn}^k \boldsymbol{\sigma}_{nM}^k \quad (5)$$

where both stiffness and compliance coefficients are employed. Subscript M denotes stress from an assumed model. The relations between the arrays of coefficients of the two forms of Hooke's law are easily found:

$$\boldsymbol{C}_{pp}^k = \tilde{\boldsymbol{C}}_{pp}^k - \tilde{\boldsymbol{C}}_{pn}^k \left(\tilde{\boldsymbol{C}}_{nn}^k\right)^{-1} \tilde{\boldsymbol{C}}_{np}^k, \qquad \boldsymbol{C}_{pn}^k = \tilde{\boldsymbol{C}}_{pn}^k \left(\tilde{\boldsymbol{C}}_{nn}^k\right)^{-1}$$

$$\boldsymbol{C}_{np}^k = -\left(\tilde{\boldsymbol{C}}_{nn}^k\right)^{-1} \tilde{\boldsymbol{C}}_{np}^k, \qquad \boldsymbol{C}_{nn}^k = \left(\tilde{\boldsymbol{C}}_{nn}^k\right)^{-1}$$

where superscript -1 indicates the inverse of a square array.

The strain components $\boldsymbol{\epsilon}_p^k = \{\epsilon_{xx}^k, \epsilon_{yy}^k, \epsilon_{xy}^k\}$ and $\boldsymbol{\epsilon}_n^k = \{\epsilon_{xz}^k, \epsilon_{yz}^k, \epsilon_{zz}^k\}$ are linearly related to the displacements $\boldsymbol{u}^k = \{u_x^k, u_y^k, u_z^k\}$ according to the following geometrical relations:

$$\boldsymbol{\epsilon}_{pG}^k = \boldsymbol{D}_p \boldsymbol{u}^k, \qquad \boldsymbol{\epsilon}_{nG}^k = \boldsymbol{D}_n \boldsymbol{u}^k \quad (6)$$

where $\boldsymbol{D}_p$ and $\boldsymbol{D}_n$ are in-plane and out-of-plane differential operators, respectively. Explicit forms of the introduced arrays are provided in the Appendix.

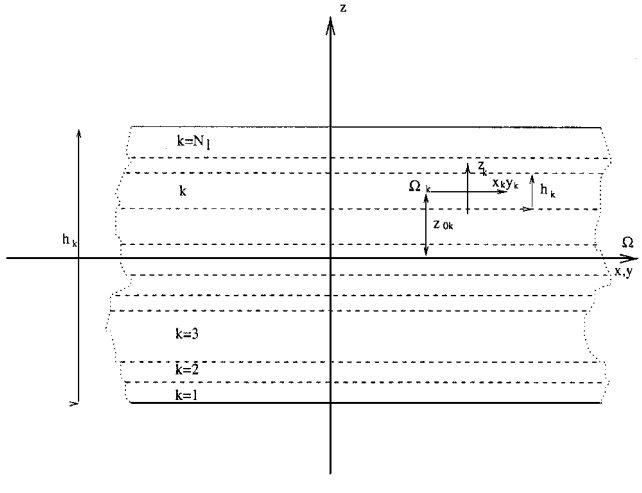

Fig. 1 Geometry and notations in a multilayered plate.

Temperature Profile with Plate-Thickness

A laminated plate, made of N_l orthotropic layers is considered (Fig. 1). Here x, y, z is a system of Cartesian coordinates and a, b, and h are the plate dimensions with respect the defined coordinates. The principal material directions of the constitutive layers coincide with the geometric axes. As done by Tungikar and Rao,[7] the attention is restricted to the particular case in which the multilayered plate is subjected to the following thermal boundary conditions:

$$T = 0 \qquad \text{at} \qquad x = 0, \quad y = 0, b$$

$$T = T_b \sin(m\pi/a)x \sin(m\pi/b)y \qquad \text{at} \qquad z = -h/2$$

$$T = T_t \sin(m\pi/a)x \sin(m\pi/b)y \qquad \text{at} \qquad z = h/2 \quad (7)$$

where m and n are the wave numbers along the plate width and length a and b, respectively. Continuity conditions for the temperature and heat flux q_z in the thickness direction, at the each k-layer interface is

$$T^k = T^{k+1}, \qquad q^k = T^{k+1}, \qquad k = 1, \quad N_l - 1 \quad (8)$$

where the relation between flux and temperature is

$$q_z^k = K_3^k \frac{\partial T^k}{\partial z} \tag{9}$$

In which $K_3 = K_z$ is the thermal conductivity of the k layer in the z direction. The differential Fourier equation of heat conduction for a homogeneous orthotropic is

$$K_1 \frac{\partial^2 T}{\partial x^2} + K_2 \frac{\partial^2 T}{\partial y^2} + K_3 \frac{\partial^2 T}{\partial z^2} = 0 \tag{10}$$

where K_1 and K_2 are the thermal conductivities in the in-plane x and y directions.

The set of governing equations can be solved as follows. The variables are separated, and the in-plane boundary conditions are satisfied by assuming the following temperature field:

$$T(x, y, z) = f(z) \sin(m\pi/a)x \sin(m\pi/b)y \tag{11}$$

where $f(z)$ is

$$f(z) = T_0 e^{sz} \tag{12}$$

T_0 is a constant and s is a parameter. Substituting Eq. (11) in the Fourier equation and solving, one gets the two roots

$$s_{1,2} = \pm\sqrt{\frac{K_1(m/\pi a)^2 + K_2(n/\pi b)^2}{K_3}} \tag{13}$$

therefore,

$$f(z) = T_{01} e^{s_1 z} + T_{02} e^{s_1 z} \tag{14}$$

or

$$f(z) = C_1^k \cosh s_1 z + C_2^k \sinh s_1 z \tag{15}$$

The solution for a typical layer k is, therefore, written as

$$T_c(z) = T^k = \left(C_1^k \cosh s_1 z + C_2^k \sinh s_1 z\right) \sin(m\pi/a)x \sin(m\pi/b)y \tag{16}$$

The $2 \times N_l$ constants C_1^k and C_2^k are determined by imposing the earlier written continuity conditions for flux q_z and temperature at $N_l - 1$ interfaces, for example, Eq. (8) along with the two additional conditions on top–bottom surface for T.

To preserve consistency with the employed plate theories (see next section) and without losing generality, the calculated temperature $T_a(z)$ given by Eqs. (16) has been expressed by using the same base function employed for transverse stress and diplacement variables,

$$T^k(x, y, z) = F_t T_t^k + F_b T_b^k + F_2 T_2^k = F_\tau T_\tau^k \tag{17}$$

This formula will be made clear in the next section.

Considered Plate Theories

The whole plate modelings considered are described. Indicial notation, subscripts and superscripts, have been used extensively to handle the presented derivations in a concise manner and to make the formulas suitable for the related computer implementations. For the sake of completeness, the paper provides some derivations and formulas that were given previously.[14,20,21]

Classical Theories Based on PVD

Classical plate theories, which are herein variationally formulated on the basis of PVDs, assume a certain expansion in terms of introduced displacement variables in the z direction. This can be done in ESL models (ESLMs) or the LW framework.

ESLMs

This subsection describes classical ESL based on PVD (ED) linear (ED1), parabolic (ED2), cubic (ED3), and fourth-order (ED4) models. According to ESLM formulation the displacement variables assume the same values in each layer. If Taylor-type expansion is employed, the displacement field is

$$\boldsymbol{u} = \boldsymbol{u}_0 + z^r \boldsymbol{u}_r, \qquad r = 1, 2, \ldots, N \tag{18}$$

N is a free parameter of the model. In contrast to N^*, N does not denote the number of terms but the order of the expansion. The repeated indices r are summed over their ranges. Subscript 0 denotes values related to the plate reference surface Ω. Here, $\boldsymbol{u}_r$ are linear and higher-order terms. If a generic set of base function $F^r(z)$ is introduced, the preceding expansion can be rewritten as follows:

$$\boldsymbol{u} = F^r(z)\boldsymbol{u}_r, \qquad r = 0, 1, 2, \ldots, N \tag{19}$$

To handle all of the modelings in a unified manner, we will use the following notations:

$$\boldsymbol{u} = F_t \boldsymbol{u}_t + F_b \boldsymbol{u}_b + F_r \boldsymbol{u}_r = F_\tau \boldsymbol{u}_\tau$$
$$\tau = t, b, r, \qquad r = 1, 2, \ldots, N \tag{20}$$

Subscript b denotes values related to the plate reference surface Ω ($\boldsymbol{u}_b = \boldsymbol{u}_0$) whereas subscript t refers to highest-order terms. For the case of Taylor-type expansion, the introduced base function holds:

$$F_b = 1, \qquad F_t = z^{N+1}, \qquad F_r = z^r, \qquad r = 1, 2, \ldots, N \tag{21}$$

For instance, first shear deformation theory (FSDT) corresponds to the $r = 0$ case with $u_{zt} = 0$. Shear correction factors χ can be used for FSDT cases, in particular classical lamination theory (CLT) results can be numerically achieved by implementing a penalty technique on χ. In fact, $\chi = \infty$ corresponds to CLT analysis. Three cases of shear correction factors will be considered in the numerical analysis. Other examples of Eq. (18)-type theory are found in Refs. 22 and 23.

ESLMs Including Zigzag

This subsection describes ED, accounting for zigzag linear (EDZ1), parabolic (EDZ2), cubic (EDZ3), and fourth-order (EDZ4) models. The zigzag form of the displacements fields can be reproduced in an equivalent single-layer description on generalization of Murakami's idea.[24] This idea simply consists of adding a zigzag term into a classical Taylor-type expansion. According to Ref. 24, the displacement model is generalized in the form

$$\boldsymbol{u} = \boldsymbol{u}_0 + (-1)^k \zeta_k \boldsymbol{u}_Z + z^r \boldsymbol{u}_r, \qquad r = 1, 2, \ldots, N \tag{22}$$

Subscript z refers to the introduced zigzag term. Higher-order distributions in the z direction are introduced by the r polynomials. In a unified form, the displacement model is, therefore, rewritten as

$$\boldsymbol{u} = F_t \boldsymbol{u}_t + F_b \boldsymbol{u}_b + F_r \boldsymbol{u}_r = F_\tau \boldsymbol{u}_\tau$$
$$\tau = t, b, r, \qquad r = 1, 2, \ldots, N \tag{23}$$

Subscript b denotes values related to the plate reference surface Ω ($\boldsymbol{u}_b = \boldsymbol{u}_0$) and subscript t now refers to the introduced zigzag term ($\boldsymbol{u}_t = \boldsymbol{u}_Z$). The functions F_τ assume the following explicit form:

$$F_b = 1, \qquad F_t = (-1)^k \zeta_k, \qquad F_r = z^r, \qquad r = 1, 2, \ldots, N \tag{24}$$

Note that F_t assumes the values ± 1 in correspondence to the bottom and the top interface of the k layer (Fig. 2a). Transverse normal stress effect will be outlined by forcing u_z constant. This will be denoted by adding the letter d at the end of the correspondent acronyms. These theories discard interlaminar equilibria but take into account zigzag

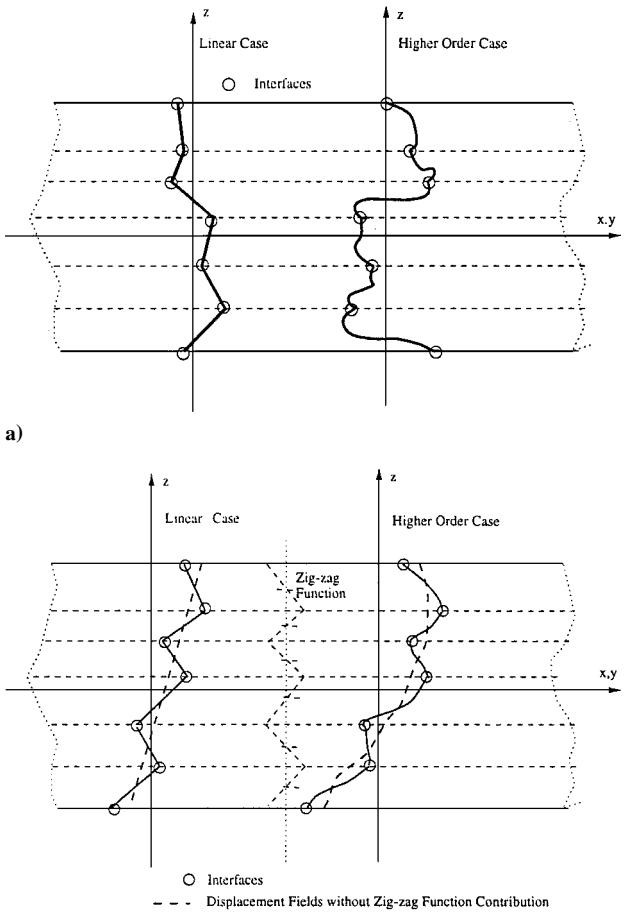

Fig. 2 Displacement and stress fields for the considered plate theories.

effects. A particular case of the theory EDZ3 has been employed in Ref. 15.

LW Theories

This subsection describes LW classical, based on PVD (LD) linear (LD1), parabolic (LD2), cubic (LD3), and fourth-order (LD4) theories. LW description requires assuming independent displacement variables in each k layer. The thickness expansion used for ESLM cases Eqs. (23) is not convenient for the LW description. Interlaminar continuity conditions can be more conveniently imposed by employing interface values in the thickness expansion. Therefore, the LW description is written according to the following expansion:

$$\boldsymbol{u}_{nM}^k = F_t \boldsymbol{u}_{nt}^k + F_b \boldsymbol{u}_{nb}^k + F_r \boldsymbol{u}_{nr}^k = F_\tau \boldsymbol{u}_{n\tau}^k$$

$$\tau = t, b, r, \qquad r = 2, 3, \ldots, N, \qquad k = 1, 2, \ldots, N_l \quad (25)$$

In contrast to Eqs. (23), subscripts t and b denote values related to the layer top and bottom surface, respectively. In fact, they consist of the linear part of the expansion. The thickness functions $F_\tau(\zeta_k)$ have been defined by

$$F_t = (P_0 + P_1)/2, \qquad F_b = (P_0 - P_1)/2, \qquad F_r = P_r - P_{r-2}$$

$$r = 2, 3, \ldots, N \quad (26)$$

in which $P_j = P_j(\zeta_k)$ is the Legendre polynomial of the j order defined in the ζ_k domain: $-1 \le \zeta_k \le 1$. The fourth-order case will be used in the numerical investigations. Related polynomials are

$$P_0 = 1, \qquad P_1 = \zeta_k, \qquad P_2 = \left(3\zeta_k^2 - 1\right)/2$$

$$P_3 = 5\zeta_k^3/2 - 3\zeta_k/2, \qquad P_4 = 35\zeta_k^4/8 - 15\zeta_k^2/4 + \tfrac{3}{8}$$

The chosen functions have the following properties:

$$\zeta_k = \begin{cases} 1{:}F_t = 1, & F_b = 0, & F_r = 0 \\ -1{:}F_t = 0, & F_b = 1, & F_r = 0 \end{cases} \quad (27)$$

The top and bottom values have been used as unknown variables. The interlaminar compatibility of displacement, therefore, can be easily linked:

$$\boldsymbol{u}_t^k = \boldsymbol{u}_b^{(k+1)}, \qquad k = 1, \qquad N_l - 1 \quad (28)$$

Examples of linear and higher-order fields have been plotted in Fig. 2b. These type of theories do not address interlaminar equilibria but do include zigzag description of both in-plane and out-of-plane displacements.

Mixed Theories Based on RMVT

RMVT permits one to assume two independent fields for displacement and transverse shear fields leading to a priori and complete fulfillment of the C_z^0–requirements. For the classical case, both ESLM and LW description can be adopted.

LW Cases

This subsection describes LM mixed formulation, based on RMVT (LM) linear (LM1), parabolic (LM2), cubic (LM3), and fourth-order cases. The LW description used for displacements is certainly suitable certainly for transverse stresses:

$$\boldsymbol{u}^k = F_t \boldsymbol{u}_t^k + F_b \boldsymbol{u}_b^k + F_r \boldsymbol{u}_r^k = F_\tau \boldsymbol{u}_\tau^k$$

$$\boldsymbol{\sigma}_{nM}^k = F_t \boldsymbol{\sigma}_{nt}^k + F_b \boldsymbol{\sigma}_{nb}^k + F_r \boldsymbol{\sigma}_{nr}^k = F_\tau \boldsymbol{\sigma}_{n\tau}^k$$

$$\tau = t, b, r, \qquad r = 2, 3, \ldots, N, \qquad k = 1, 2, \ldots, N_l \quad (29)$$

The top and bottom values have also been used as unknown variables. The interlaminar transverse shear and normal stress continuity, therefore, can be easily linked: $\boldsymbol{\sigma}_{nt}^k = \boldsymbol{\sigma}_{nb}^{(k+1)}$, $k = 1$, and $N_l - 1$.

ESL Cases

This subsection describes ESL mixed, based on RMVT (EM) with zigzag accounted for and interlaminar continuity (EMZC) linear (EMZC1), parabolic (EMZC2), cubic (EMZC3), and fourth-order (EMZC4) cases. To include zigzag function in the framework of ESLM analysis, the displacement field of Eq. (22) can be adopted:

$$\boldsymbol{u} = F_t \boldsymbol{u}_t + F_b \boldsymbol{u}_b + F_r \boldsymbol{u}_r = F_\tau \boldsymbol{u}_\tau$$

$$\tau = t, b, r, \qquad r = 1, 2, \ldots, N \quad (30)$$

whereas interlaminar continuous transverse shear and normal stress in the RMVT framework require reference to the LW description for transverse stresses:

$$\boldsymbol{\sigma}_{nM}^k = F_t \boldsymbol{\sigma}_{nt}^k + F_b \boldsymbol{\sigma}_{nb}^k + F_r \boldsymbol{\sigma}_{nr}^k = F_\tau \boldsymbol{\sigma}_{n\tau}^k,$$

$$\tau = t, b, r, \qquad r = 2, 3, \ldots, N, \qquad k = 1, 2, \ldots, N_l \quad (31)$$

Note that the ESLM description has been restricted to displacement variables. In practice, stress variables can be eliminated by static condensation or by employing the technique described in Ref. 9. In practice, the assumption that u_Z is k independent makes the obtained theories unable to describe accurately any effects that are dominated by the layer mechanics.

Summary of Considered Theories

Depending on the used variational statement (PVD or RMVT), variables description (LW or ESL), order of the used expansion N, inclusion or not of σ_{zz} effects, etc., a number of two-dimensional theories can be constructed on the bases of the modelings described in the preceding subsections. Acronyms will be used extensively in the numerical part to denote these theories. Figure 3 shows the acronyms have been built. For instance, both transverse stress and displacement models in each layer are introduced in the LM1–LM4 cases. Only displacement assumptions are made in the LD1–LD4 cases,

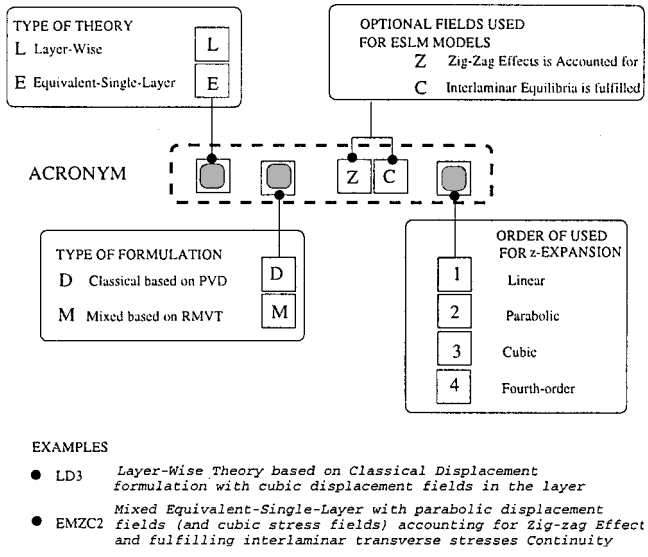

Fig. 3 Derivation of the introduced acronyms.

whereas ED1–ED4 theories refer to assumptions that are made at plate multilayer level. Parabolic transverse stress field in each layer is associated to linear zigzag diplacement field for the EMZC1 case and the fourth-order transverse stress field in each layer is associated to the cubic zigzag displacement field for the EMZC3 case.

Thermomechanical Governing Equations

The differential equations and boundary conditions governing the thermomechanical response of a layered plate for the theories described earlier have been derived previously by the author.[14] (See Ref. 14 for details.) Herein a brief description is given for completeness.

Classical Theories Based on PVD

The classical displacement approach is formulated in terms of $\boldsymbol{u}^k$ via the principle of virtual displacements that, in the static case and in presence of thermal stresses, states

$$\sum_{k=1}^{N_l} \int_{\Omega^k} \int_{A_k} \left[\delta \boldsymbol{\epsilon}_{pG}^{k\,T} \left(\boldsymbol{\sigma}_{p\,H_d}^k - \boldsymbol{\sigma}_{p\,T}^k \right) + \delta \boldsymbol{\epsilon}_{nG}^{k\,T} \left(\boldsymbol{\sigma}_{n\,H_d}^k - \boldsymbol{\sigma}_{n\,T}^k \right) \right] \mathrm{d}\Omega^k \, \mathrm{d}z = \delta L^e \tag{32}$$

where δ is the variational symbol and subscript T are transposition of arrays. A_k and V are the layer-thickness domain and volume and Ω^k is the layer middle surface bounded by Γ^k. Γ_g^k and Γ_m^k are those parts of Γ^k on which the geometrical and mechanical boundary conditions are prescribed, respectively. The variation of the internal work has been split into in-plane and out-of-plane parts and involves stress from Hooke's law and strain from geometrical relations. Here, δL_e is the virtual variation of the work made by the external-layer forces $\boldsymbol{p}^k = \{p_x^k, p_y^k, p_z^k\}$. Based on the assumed modelings, Eq. (32) leads, for each k layer, to the following equilibrium equations on Ω^k:

$$\delta \boldsymbol{u}_\tau^k : -\boldsymbol{D}_p^T \left(\mathcal{R}_{pH_d}^{k\tau} - \mathcal{R}_{pT}^{k\tau} \right) + \mathcal{R}_{nH_d}^{k\tau_z} + \mathcal{R}_{nT}^{k\tau_z} - \boldsymbol{D}_{n\Omega}^T \left(\mathcal{R}_{nH_d}^{k\tau} - \mathcal{R}_{nT}^{k\tau} \right) = \boldsymbol{p}_\tau^k \tag{33}$$

and the boundary conditions on Γ^k are as follows.

Geometrical on Γ_g^k:

$$\boldsymbol{u}_\tau^k = \bar{\boldsymbol{u}}_\tau^k \tag{34}$$

Mechanical on Γ_m^k:

$$\boldsymbol{I}_p^T \left(\mathcal{R}_{pH_d}^{k\tau} - \mathcal{R}_{pT}^{k\tau} \right) + \boldsymbol{I}_{n\Omega}^T \left(\mathcal{R}_{nH_d}^{k\tau} - \mathcal{R}_{nT}^{k\tau} \right) = \boldsymbol{I}_p^T \left(\bar{\mathcal{R}}_{pH_d}^{k\tau} - \bar{\mathcal{R}}_{pT}^{k\tau} \right) + \boldsymbol{I}_{n\Omega}^T \left(\bar{\mathcal{R}}_{nH_d}^{k\tau} - \bar{\mathcal{R}}_{nT}^{k\tau} \right)$$

The following stress layer resultants are defined:

$$\left(\mathcal{R}_{pH_d}^{k\tau}, \mathcal{R}_{nH_d}^{k\tau}, \mathcal{R}_{nH_d}^{k\tau_z} \right) = \int_{A_k} \left(F_\tau \boldsymbol{\sigma}_{pH_d}^k, F_\tau \boldsymbol{\sigma}_{nH_d}^k, F_{\tau_z} \boldsymbol{\sigma}_{nH_d}^k \right) \mathrm{d}z$$

$$\left(\mathcal{R}_{pT}^{k\tau}, \mathcal{R}_{nT}^{k\tau}, \mathcal{R}_{nT}^{k\tau_z} \right) = \int_{A_k} \left(F_\tau \boldsymbol{\sigma}_{pT}^k, F_\tau \boldsymbol{\sigma}_{nT}^k, F_{\tau_z} \boldsymbol{\sigma}_{nT}^k \right) \mathrm{d}z \tag{35}$$

The overbar denotes imposed values at the boundary. The complete set of equations for the N_l layers could be written simply by expanding over their ranges the introduced subscripts and superscripts.[14] The continuity conditions for the displacement variables with correspondence to each interface are introduced by writing multilayer equations.

Advanced Mixed Theories Based on RMVT

In the case of mixed-plate theories, equilibrium and compatibility are both formulated in terms of the $\boldsymbol{u}^k$ and $\boldsymbol{\sigma}_n^k$ unknowns via Reissner's variational equation[25,26] (also see Ref. 24)

$$\sum_{k=1}^{N_l} \int_{\Omega^k} \int_{A_k} \left\{ \delta \boldsymbol{\epsilon}_{pG}^{k\,T} \left(\boldsymbol{\sigma}_{p\,H}^k - \boldsymbol{\sigma}_{p\,T}^k \right) + \delta \boldsymbol{\epsilon}_{nG}^{k\,T} \boldsymbol{\sigma}_{n\,M}^k + \delta \boldsymbol{\sigma}_{n\,M}^{k\,T} \left[\boldsymbol{\epsilon}_{n\,G}^k - \left(\boldsymbol{\epsilon}_{n\,H}^k - \boldsymbol{\epsilon}_{n\,T}^k \right) \right] \right\} \mathrm{d}\Omega^k \, \mathrm{d}z = \delta L^e \tag{36}$$

The left-hand side includes the variations of the internal work in the plate: The first two terms come from the displacement formulation and lead to variationally consistent equilibrium conditions; the third mixed term variationally enforces the compatibility of the transverse strain components.

When the definition of virtual variations for the unknown stress and displacement variables is imposed, the differential system of governing equations and related boundary conditions for the k layer are obtained in terms of the introduced stress and strain resultants.

The equilibrium equations on Ω^k are

$$\delta \boldsymbol{u}_\tau^k : -\boldsymbol{D}_p^T \left(\mathcal{R}_{pH}^{k\tau} - \mathcal{R}_{pT}^{k\tau} \right) + \mathcal{R}_{nM}^{k\tau_z} - \boldsymbol{D}_{n\Omega}^T \mathcal{R}_{nM}^{k\tau} = \boldsymbol{p}_\tau^k \tag{37}$$

The constitutive equations on Ω^k are

$$\delta \boldsymbol{\sigma}_{n\tau}^k : \mathcal{S}_{nG}^{k\tau} - \left(\mathcal{S}_{nH}^{k\tau} - \mathcal{S}_{nT}^{k\tau} \right) = 0 \tag{38}$$

The boundary conditions on Γ^k are as follows.

Geometrical on Γ_g^k:

$$\boldsymbol{u}_\tau^k = \bar{\boldsymbol{u}}_\tau^k \tag{39a}$$

Mechanical on Γ_m^k:

$$\boldsymbol{I}_p^T \mathcal{R}_{pH}^{k\tau} + \boldsymbol{I}_{n\Omega}^T \mathcal{R}_{nM}^{k\tau} = \boldsymbol{I}_p^T \bar{\mathcal{R}}_{pH}^{k\tau} + \boldsymbol{I}_{n\Omega}^T \bar{\mathcal{R}}_{nM}^{k\tau} \tag{39b}$$

Further stress and strain layer resultants have been introduced:

$$\left(\mathcal{R}_{pH}^{k\tau}, \mathcal{R}_{nM}^{k\tau}, \mathcal{R}_{nM}^{kt_z}, \mathcal{S}_{nG}^{k\tau}, \mathcal{S}_{nH}^{k\tau}, \mathcal{S}_{nT}^{k\tau} \right) = \int_{A_k} \left(F_\tau \boldsymbol{\sigma}_{pH}^k, F_\tau \boldsymbol{\sigma}_M^k, F_{\tau_z} \boldsymbol{\sigma}_M^k, F_\tau \boldsymbol{\epsilon}_{nG}^k, F_\tau \boldsymbol{\epsilon}_{nH}^k, F_\tau \boldsymbol{\epsilon}_{nT}^k \right) \mathrm{d}z \tag{40}$$

The preceding layer equations can be obtained at the multilayered level by enforcing the continuity conditions for the displacement and transverse stress variables with correspondence to each interface.

Closed-Form Solutions

Exact, closed-form solutions of the derived system of differential equations that govern the thermomechanical response of a generally laminated multilayered plate are not available. Approximate solution procedures could be conveniently implemented for this purpose.[9] The particular case in which the material has the properties $\tilde{C}_{16} = \tilde{C}_{26} = \tilde{C}_{36} = \tilde{C}_{45} = 0$ has been considered here. In this

case, Navier-type closed-form solutions can be found by assuming the following harmonic forms for the applied mechanical and thermal loadings and unknown variables:

$$\left(u^k_{x_\tau}, \sigma^k_{xz_\tau}, p^k_{x_\tau}\right) = \sum_{m,n} \left(U^k_{x_\tau}, S^k_{xz_\tau}, P^k_{x_\tau}\right) \cos\frac{m\pi x}{a} \sin\frac{n\pi y}{b}$$

$$\left(u^k_{y_\tau}, \sigma^k_{yz_\tau}, p^k_{y_\tau}\right) = \sum_{m,n} \left(U^k_{y_\tau}, S^k_{yz_\tau}, P^k_{y_\tau}\right) \sin\frac{m\pi x}{a} \cos\frac{n\pi y}{b}$$

$$\left(u^k_{z_\tau}, \sigma^k_{zz_\tau}, p^k_{z_\tau}\right) = \sum_{m,n} \left(U^k_{z_\tau}, S^k_{zz_\tau}, P^k_{z_\tau}\right) \sin\frac{m\pi x}{a} \sin\frac{n\pi y}{b}$$

$$T = T(z) \sin\frac{m\pi x}{a} \sin\frac{n\pi y}{b} \tag{41}$$

which correspond to simply supported boundary conditions. Here m and n are wave numbers in the x and y directions, respectively. The upper case sumbols on the right-hand side are corresponding maximum amplitudes. On substitution of Eqs. (41), the governing equations given in the preceding subsections assume the form of a linear system of algebraic equations, whose solutions are discussed in the next section.

Numerical Illustrations and Discussion

A large investigation has been conducted to evaluate the temperature profiles of layered plates and their influence on plate response as well as on the accuracy of two-dimensional modelings. Stress and displacement fields are computed by taking several temperature fields as well as multilayered layouts and geometries into account. More than 20 plate theories are compared. The most significant results are selected and presented in the next sections. Only thermal loadings are considered. To be consistent with a given plate theory, the calculated temperature profile in Eq. (16) has always been introduced, referring to the same expansion used for $\boldsymbol{u}$ and $\boldsymbol{\sigma}_n$.

Description of Four Sample Problems

The numerical results are related to four sample problems, whose data are shown and described in Figs. 4 and 5 and Table 1. The usual notations have been used as far as the mechanical properties are concerned (see Ref. 27). The four sample problems are 1) one-layered aluminum 5086 plate, 2) three-layered graphite–epoxy plate according to Tungikar and Rao,[7] 3) three-layered sandwich plate, and 4) three-layered graphite–epoxy plate according to Bhaskar et al.[8] The top/bottom plate surface temperature always refers to the environmental temperature T_e. The displacement and stresses have been adimensioned as follows:

$$u_x = U_x, \qquad u_z = U_z/(a/h)^2, \qquad \sigma_{xx} = S_{xx}$$

$$\sigma_{xz} = S_{xz}, \qquad \sigma_{zz} = S_{zz}$$

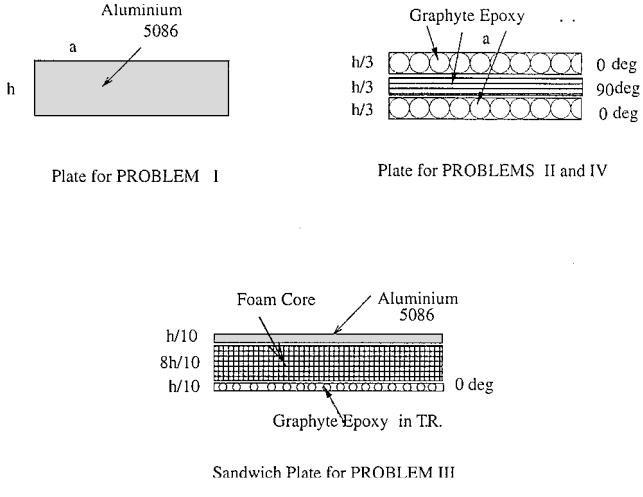

Fig. 4 Layout of plate problems 1–4.

Table 1 Thermomechanical properties of considered materials

Property	Value
Aluminum 5086	
E, N/mm^2	70,300
ν	0.33
α, °C^{-1}	24.E−6
K, W/m °C	130
Graphite–epoxy (Ref. 7)	
E_L, N/mm^2	172.72E−6
E_T, N/mm^2	E_3 6.909E−6
G_{LT}, N/mm^2	3.45E−6
G_{TT}, N/mm^2	1.38E−6
$\nu_{LT} = \nu_{TT}$	0.25
α_L, °C^{-1}	0.57E−6
α_T, °C^{-1}	35.6E−6
K_L, W/m °C	36.42
K_T, W/m °C	0.96
Graphite–epoxy (Ref. 8; nondimensionalized)	
E_L/E_T	25
G_{LT}/E_T	0.5
G_{TT}/E_T	0.3
$\nu_{LT} = \nu_{TT}$	0.25
α_T/α_L	1125
K_L, K_T	See Ref. 7
Sandwich core	
E, G	0.001 × (E, G)[a]
α, K	1000 × (α, K)[a]

[a]Values of aluminum 5086.

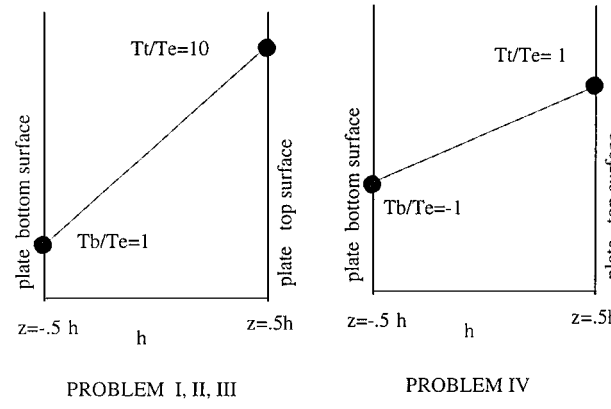

Fig. 5 Temperature at the top/bottom plate surfaces for problems 1–4, linear case $T_a(z)$ shown.

where U_x, U_z, S_{xx}, S_{xz}, are S_{zz} are the maximum values (amplitudes of their harmonic distributions) of the related displacements and stresses in the plate in Eqs. (41).

Temperature Profiles

The heat conduction problem has been solved for the proposed sample problems. The results are shown in Fig. 6, which shows the effects of plate/thickness ratio a/h on $T_c(z)$. The following comments can be made on this Fig. 6. 1) Thick and moderately thick plates exhibit an effective profile $T_c(z)$, which differs considerably from $T_a(z)$. 2) The linear form of temperature profile $T_a(z)$ is approached only for the thin-plate geometry. 3) The differences between the linear and effective form of the temperature profiles are more evident in the case of layered plates, as well as in the case of problems 1–3 compared to problem 4.

A general conclusion is that thick plates ($a/h < 10$) show a temperature profile $T_c(z)$, whose accurate description could be acquired using a very high-order expansion for the polynomials F_τ in Eq. (17). Analyses conducted by the author, which are not documented here, have shown that higher than five-order ESLM-type expansions should be used to have an acceptable description of T_c in the laminates. Much lower-order (linear or parabolic) expansion could be sufficient if an LW description is instead used. The author's opinion

is that it does not appear reasonable to employ such a high-order ESLM expansion if the same expansion is not used in the assumed displacement and stress fields. In other words, a higher-order plate theory is required to capture correctly the effects of a higher-order through-the-thickness variation of thermal loadings.

Effect of Temperature Profile on Plate Response

The influence of temperature profiles on the response of the introduced sample problems has been dealt with by implementing an LW mixed theory with four-order polynomials in each layer for both the displacements and transverse shear and normal stresses (LM4) (see the third section).

Table 2 deals with the Bhaskar et al. thermomechanical problem,[8] problem 4. Transverse displacements and transverse shear stresses are compared for very thick $a/h=2$, thick $a/h=4$, moderately thick $a/h=10$, and thin plates $a/h=100$. In Ref. 8, attention was restricted to the $T_a(z)$ case. Table 2 confirms the effectiveness of LM4 plate theories to give a three-dimensional description of displacement and stress fields (also Ref. 14). Further results are given in Table 3 and Figs. 7–9 show stress or displacement components vs plate thickness. Tranverse stresses have been calculated by postprocessing integration of three-dimensional indefinite equilibrium equations. A few comments on these results follow: 1) The LM4 results (Table 2) could reasonably be kept as a reference solution for those problems in which three-dimensional analysis is not available, such as problems 1–3. 2) Table 2 and Fig. 7 show that large differences are obtained by enforcing a T_a–type thermal loadings in thick plates. A large error should be registered for transverse

Table 2 Influence of temperature profile on the response plate problem 4, LM4 analysis

	u_z at $z=h/2$			σ_{xx} at $z=\mp h/2$			σ_{xz} at $z=\mp h/6$		
a/h	T_a[a]	T_a	T_c	T_a[a]	T_a	T_c	T_a[a]	T_a	T_c
2	96.79	96.79	75.60	1390	1390	939.4	63.92	63.92	32.19
4	42.69	42.69	37.91	1183	1183	975.9	84.81	84.81	71.19
10	17.39	17.39	16.92	1026	1026	982.0	60.54	60.64	58.65
20	12.12	12.12	12.03	982.0	982	970.5	33.98	33.98	33.71
50	10.50	10.50	10.48	967.5	967.5	965.7	14.07	14.07	14.06
100	10.26	10.26	10.26	965.4	965.4	965.0	7.073	7.073	7.071

[a]Three-dimensional analysis by Bhaskar et al.[8]

Table 3 Influence of temperature profile on the response of thick and thin plates, problems 2 and 3 results, LM4 analysis

	Problem 2		Problem 3	
a/h	T_a	T_c	T_a	T_c
		u_z at $z=h/2$		
2	0.4164E−4	0.2130E−4	0.1946E−1	0.1466E−1
4	0.1381E−4	0.9355E−5	0.1594E−1	0.1444E−1
10	0.4087E−5	0.3766E−5	0.3427E−2	0.3368E−2
20	0.2454E−5	0.2419E−5	0.8413E−3	0.8375E−3
50	0.1977E−5	0.1974E−5	0.1506E−3	0.1505E−3
100	0.1908E−5	0.1907E−5	0.6885E−3	0.6884E−4
		Transverse shear stress σ_{xz}[a]		
2	−0.2391E+3	0.2686E+2	−0.3520E+2	−0.2149E+2
	0.3602E+3	0.3680E+2	0.8176E+0	0.4016E+1
4	−0.7482E+2	0.3672E+2	−0.1621E+2	−0.1403E+1
	0.2366E+3	0.1004E+3	0.3043E+1	0.3304E+1
10	−0.4522E+1	0.1359E+2	−0.5327E+1	−0.5194E+1
	0.1201E+3	0.9857E+2	0.1228E+1	0.1246E+0
20	−0.1322E+1	0.4208E+1	−0.2763E+1	−0.2746E+1
	0.6359E+2	0.6020E+2	0.4088E+0	0.4117E+0
50	0.9933E+0	0.1193E+1	−0.1370E+1	−0.1368E+1
	0.2589E+2	0.2566E+2	−0.1067E+0	−0.1063E+0
100	0.5311E+0	0.5564E+0	−0.7736E+0	−0.7735E+0
	0.1298E+2	0.1295E+2	−0.1421E+0	0.1420E+0

[a]Problem 2 T_a and T_c, $z\mp h/6$; problem 3 T_a and T_c, $z=\mp 9/10h$.

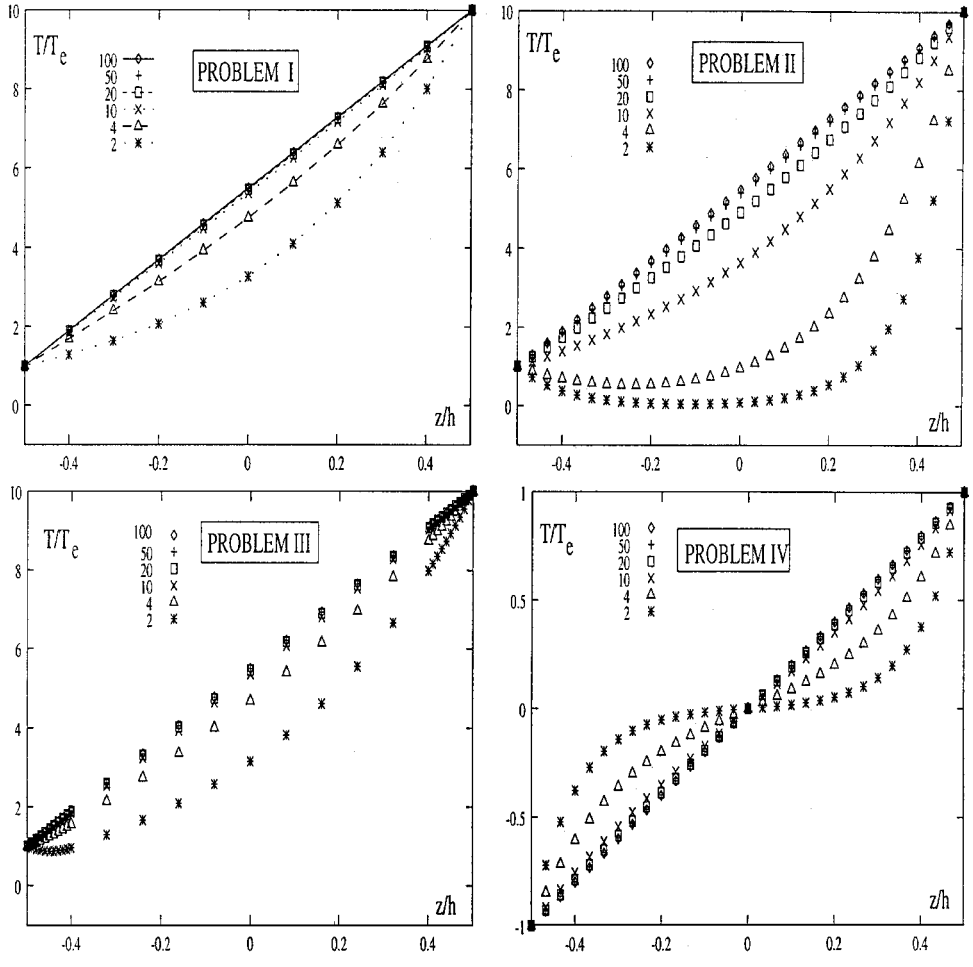

Fig. 6 Temperature profiles $T(z)$ for different plate thickness ratios a/h.

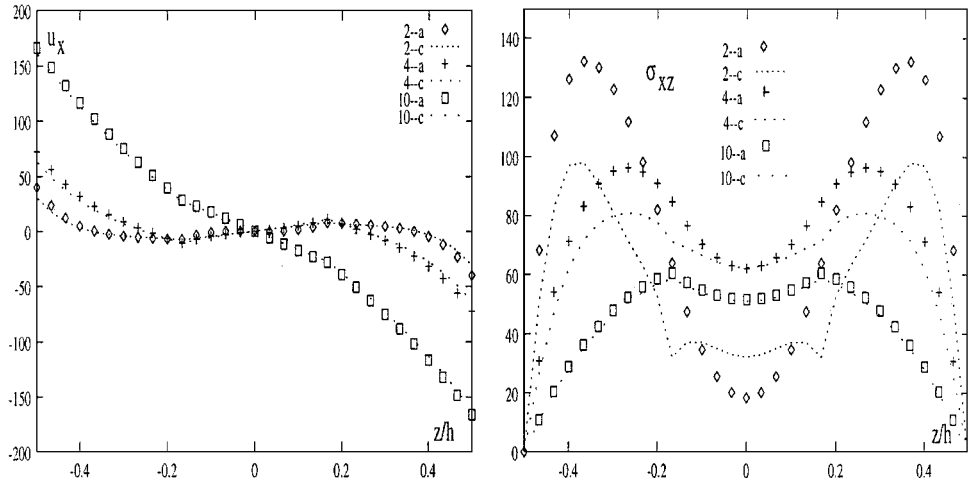

Fig. 7 Influence of thickness ratio *a/h* on displacement and transverse stress fields: problem 4, LM4 analysis.

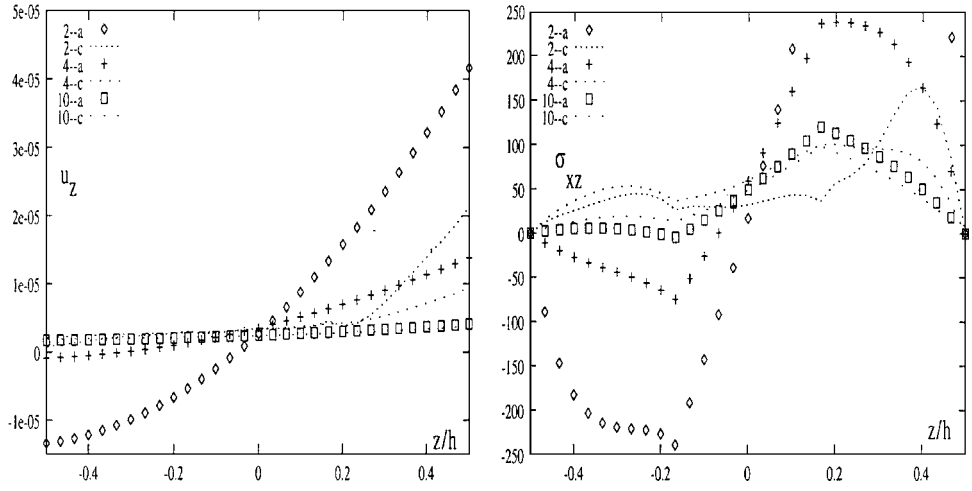

Fig. 8 Influence of thickness ratio *a/h* on displacement and transverse stress fields: problem 2, LM4 analysis.

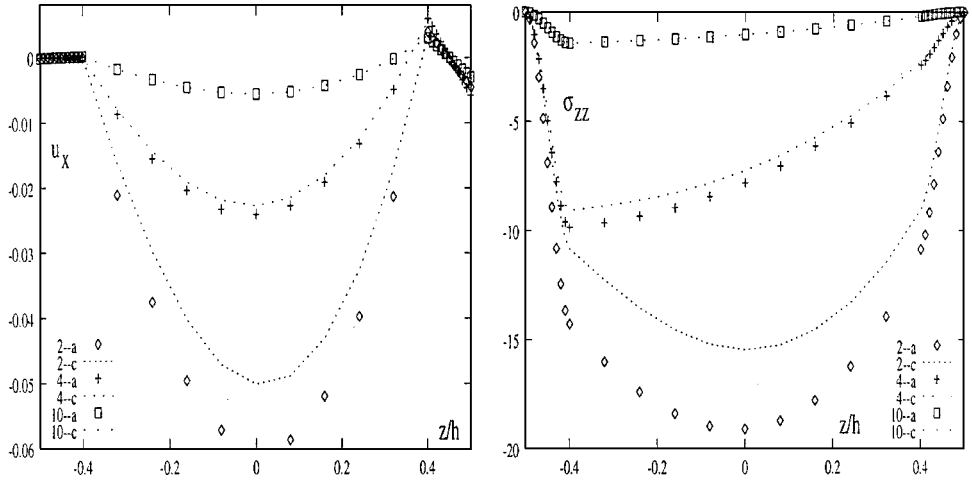

Fig. 9 Influence of thickness ratio *a/h* on displacement and transverse stress fields: problem 3, LM4 analysis.

shear stresses when compared to displacement evaluations (errors of about 50% in the $a/h = 2$ case). Much higher differences should be registered for problems 2 and 3 analysis (Table 4 and Figs. 7 and 8). These latter results show that the sign of stresses can be wrongly predicted by enforcing the T_a profile (which could happen until $a/h \leq 20$). 3) The $T_a(z)$ and $T_c(z)$ results merge in thin-plate cases. 4) Figures 7–9 show that the stress and displacement fields mostly exhibit an LW form.

Effect of Temperature Profile on Accuracy of Classical and Advanced Plate Theories

The overall two-dimensional theories described in the fourth section have been implemented and compared for the sample problems here proposed. Problem 1, which deals with a one-layered plate, does not require LW analysis nor application of the mixed theory. The LD4 results should in fact coincide with the corresponding ED4 results. However, for those thick-plate problems in which very

high expansion is required to emulate correctly the calculated profile T_c, a difference could appear. Such a difference should be put down to the different manner in which the Taylor expansion related to the ED4 model and the Legendre-type expansion related to LM4 plate model emulate T_c in Eq. (16). This conclusion makes it clear that the differences between results, which will be compared in the next discussions, are not only due to the limitation of a given plate theories, but also to the difficulties of a given theory to emulate the effective temperature profile in Eq. (16). (Also see the comments made at the end of the second subsection of this section.)

Problem 1 results are given in Table 4 and Fig. 10, which compare classical (CLT and FSDT) and refined (ED1–ED4) theories that have here been formulated on the basis of PVD. The thickness deformation effects ϵ_{zz} have been investigated by quoting ED1d–ED4d results (where d denotes that transverse normal strains are discarded by forcing u_z to be constant). ED1d should then coincide with the classical FSDT, which relies on the well know Reissner–Mindlin type hypotheses, whereas the CLT, which is based on Kirchhoff's well-known plate assumptions, has been obtained from the ED1 theory, by implementing a penalty method on shear correction factor χ (Ref. 14.) The following comments can be made: 1) ED4, ED3, and ED2 results merge for thin plates in both cases of assumed T_a and calculated T_c temperature profiles. 2) The differences between transverse displacement u_z obtained from different plate theories (ED1–ED4) could be negligible if compared to the differences that different temperature profiles (T_a and T_c) show for the same plate theories. 3) The ED1 results do not work well for thin plates. This phenomenon is basically because the considered temperature loading possesses at least a linear z distribution in the plate. As a consequence, the related transverse normal thermal strains are linear. Such a linear distribution requires at least a quadratic transverse displacement field u_z in each layer, which is not considered in the ED1 analysis. For the same reasons, the ED1d–ED4d as well as CLT and FSDT analyses are inaccurate; these neglect any transverse normal strains effects, in both thick and thin cases. In particular, u_z is not affected by a/h or by the plate theory in the case of assumed temperature profile T_a. Further insight into this subject is given in Ref. 14. The differences in the results related to the T_c cases are also due to the already discussed difficulties that a given plate theory could show to describe correctly Eq. (16).

The results related to problems 2–4 are given in Tables 5 and 6 and Figs. 11–15. LW, as well as classical and mixed analyses, are compared in these cases. A few conclusions follow:

Table 4 Problem 1, comparison of theories, transverse displacement u_z at $z = h/2$

		a/h			
Theory	$T(z)$	2	4	10	100
LD4	T_a	$0.4300E-4$	$0.2182E-4$	$0.1572E-4$	$0.1457E-4$
	T_c	$0.4090E-4$	$0.2148E-4$	$0.1567E-4$	$0.1457E-4$
ED4	T_a	$0.4300E-4$	$0.2182E-4$	$0.1572E-4$	$0.1457E-4$
	T_c	$0.3588E-4$	$0.2122E-4$	$0.1571E-4$	$0.1457E-4$
ED3	T_a	$0.4292E-4$	$0.2182E-4$	$0.1572E-4$	$0.1457E-4$
	T_c	$0.3275E-4$	$0.2075E-4$	$0.1565E-4$	$0.1457E-4$
ED2	T_a	$0.4180E-4$	$0.2156E-4$	$0.1568E-4$	$0.1457E-4$
	T_c	$0.3277E-4$	$0.2028E-4$	$0.1554E-4$	$0.1456E-4$
ED1	T_a	$0.4101E-4$	$0.2703E-4$	$0.2260E-4$	$0.2173E-4$
	T_c	$0.2929E-4$	$0.2522E-4$	$0.2240E-4$	$0.2173E-4$
ED4d	T_a	$0.2172E-4$	$0.2172E-4$	$0.2172E-4$	$0.2172E-4$
	T_c	$0.2098E-4$	$0.2173E-4$	$0.2174E-4$	$0.2172E-4$
ED3d	T_a	$0.2172E-4$	$0.2172E-4$	$0.2172E-4$	$0.2172E-4$
	T_c	$0.2020E-4$	$0.2130E-4$	$0.2165E-4$	$0.2172E-4$
ED2d	T_a	$0.2172E-4$	$0.2172E-4$	$0.2172E-4$	$0.2172E-4$
	T_c	$0.1782E-4$	$0.2064E-4$	$0.2154E-4$	$0.2172E-4$
ED1d	T_a	$0.2172E-4$	$0.2172E-4$	$0.2172E-4$	$0.2172E-4$
(FSDT)	T_c	$0.1782E-4$	$0.20644-4$	$0.2154E-4$	$0.2172E-4$
ED1d$^{\chi=\infty}$	T_a	$0.2172E-4$	$0.2172E-4$	$0.2172E-4$	$0.2172E-4$
(CLT)	T_c	$0.1782E-4$	$0.2064E-4$	$0.2154E-4$	$0.2171E-4$

Table 5 Problem 3, comparison of theories, transverse displacement u_z at $z = h/2$

		a/h			
Theory	$T(z)$	2	4	10	100
LM4	T_a	$0.1369E-1$	$0.9346E-2$	$0.1927E-2$	$0.5108E-4$
	T_c	$0.1145E-1$	$0.8794E-2$	$0.1906E-2$	$0.5121E-4$
LM1	T_a	$0.1191E-1$	$0.8553E-2$	$0.1875E-2$	$0.5545E-4$
	T_c	$0.9634E-2$	$0.8009E-2$	$0.1854E-2$	$0.5558E-4$
LD4	T_a	$0.1369E-1$	$0.9346E-2$	$0.1927E-2$	$0.5108E-4$
	T_c	$0.1145E-1$	$0.8794E-2$	$0.1906E-2$	$0.5121E-4$
LD1	T_a	$0.1092E-1$	$0.8424E-2$	$0.1873E-2$	$0.5413E-4$
	T_c	$0.8845E-2$	$0.7890E-2$	$0.1851E-2$	$0.5430E-4$
EMZC3	T_a	$0.8442E-2$	$0.8214E-2$	$0.1869E-2$	$0.5001E-4$
	T_c	$0.5325E-2$	$0.7134E-2$	$0.1824E-2$	$0.5000E-4$
EMZC1	T_a	$0.5760E-3$	$0.5542E-3$	$0.4420E-3$	$0.5472E-4$
	T_c	$0.3284E-3$	$0.4717E-3$	$0.4302E-3$	$0.5471E-4$
EDZ3	T_a	$0.8213E-2$	$0.8118E-2$	$0.1865E-2$	$0.5002E-4$
	T_c	$0.5184E-2$	$0.7051E-2$	$0.1821E-2$	$0.5001E-4$
ED4	T_a	$0.2639E-2$	$0.8583E-3$	$0.1581E-3$	$0.4093E-4$
	T_c	$0.1718E-2$	$0.7546E-3$	$0.1548E-3$	$0.4092E-4$
ED1	T_a	$0.7994E-4$	$0.6648E-4$	$0.6267E-4$	$0.6195E-4$
	T_c	$0.4188E-4$	$0.5813E-4$	$0.6145E-4$	$0.6193E-4$
ED1d$^{\chi=5/6}$	T_a	$0.6210E-4$	$0.6268E-4$	$0.6286E-4$	$0.6290E-4$
(FSDT)	T_c	$0.4130E-4$	$0.5572E-4$	$0.6163E-4$	$0.6289E-4$
ED1d$^{\chi=\infty}$	T_a	$0.6290E-4$	$0.6290E-4$	$0.6290E-4$	$0.6290E-4$
(CLT)	T_c	$0.4185E-4$	$0.5592E-4$	$0.6167E-4$	$0.6210E-4$

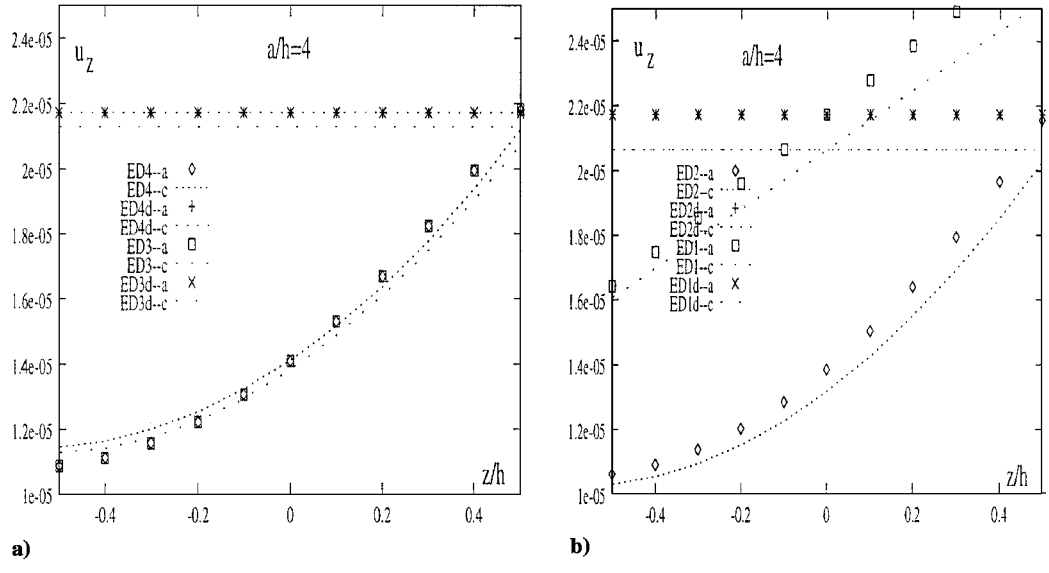

Fig. 10 Problem 1, thick plate: a) higher-order and b) lower-order theory.

Table 6 Problem 4, comparison of theories, transverse displacement $\bar{u}_z$ at $z = h/2$

		a/h			
Theory	$T(z)$	2	4	10	100
Three dimensional	T_a	96.79	42.69	17.39	10.26
	T_c	——	——	——	——
LM4	T_a	96.79	42.69	17.39	10.26
	T_c	75.60	37.91	16.92	10.26
LM1	T_a	96.86	42.62	17.36	10.33
	T_c	81.31	38.90	16.96	10.33
LD4	T_a	96.78	42.69	17.39	10.26
	T_c	75.16	37.91	16.92	10.26
LD1	T_a	89.25	41.24	17.92	10.91
	T_c	73.73	37.30	17.19	10.91
EMZC3	T_a	95.26	42.42	17.38	10.26
	T_c	40.83	30.52	15.53	10.24
EMZC1	T_a	50.82	36.65	21.63	16.16
	T_c	37.88	15.74	18.55	16.09
EDZ3	T_a	94.87	42.34	17.37	10.26
	T_c	40.82	30.49	15.52	10.24
ED4	T_a	98.22	42.05	16.90	10.25
	T_c	40.73	30.29	15.12	10.24
ED1	T_a	42.71	30.42	19.45	16.09
	T_c	3.184	13.06	16.68	16.07
ED1d$^{\chi=5/6}$ (FSDT)	T_a	44.05	32.06	20.06	16.10
	T_c	32.84	13.77	17.20	16.08
ED1d$^{\chi=\infty}$ (CLT)	T_a	16.06	16.06	16.06	16.04
	T_c	1.197	6.896	13.77	16.02

1) Better evaluations are obtained for mixed theories than for classical ones. Such a result confirms the effectiveness of Reissner's theorem to analyze the thermomechanical response of multilayered structures.

2) Both higher-order (LM4 and LD4) and lower-order (LM1 and LD1) LW theories lead to excellent results in the case of assigned temperature profile T_a (Table 6). A quite different response is found in the case of calculated profile T_c for thick-plate geometries. This is due to the already discussed difficulties that a lower-order LW expansion could meet to describe correctly the $T(z)$ profile originated by Eq. (16). This is much more evident in the case of equivalent single-layer plate theories and unsymmetrically laminated sandwich plates (Table 5).

3) Advanced zigzag theories, such as EMZC3 and EDZ3 theories, although working very well in thick plates loaded by $T_a(z)$ (as underlined in Ref. 15), cannot be used if the calculated (effective) temperature profile T_c is employed.

4) Higher differences are registered among the different theories in correspondence to the sandwich interfaces as well as for problems 2 and 3 compared to problem 4 (which has an antisymmetric temperature profile). In some cases, the sign of the transverse shear stresses can be wrongly predicted.

5) Figure 15 shows that inescapable errors involved in the integration of the three-dimensional equilibrium equations (which consist of a postprocessing procedure) can lead to violation of the zero-bottom homogeneous conditions for the transverse normal stresses.

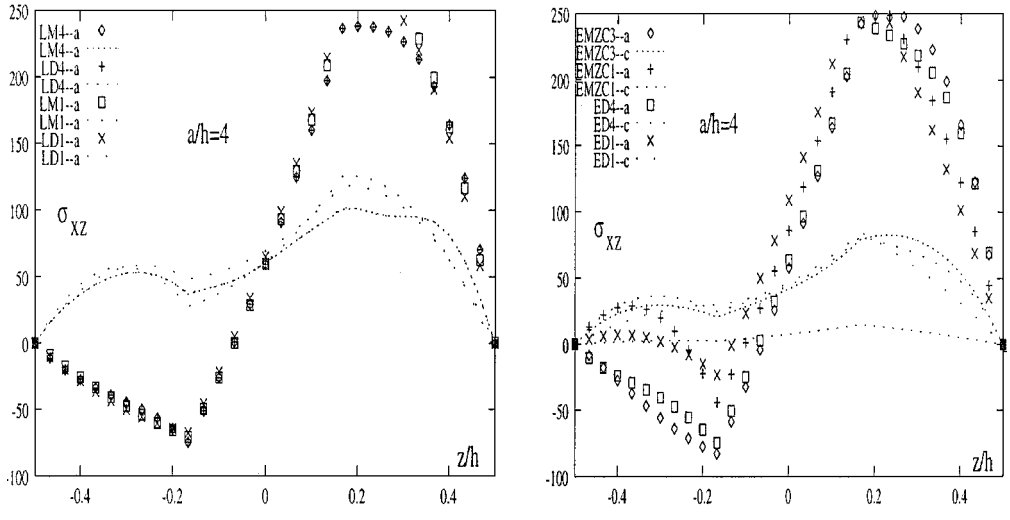

a) b)

Fig. 11 Problem 2, thick plate: a) LW and b) ESL theory.

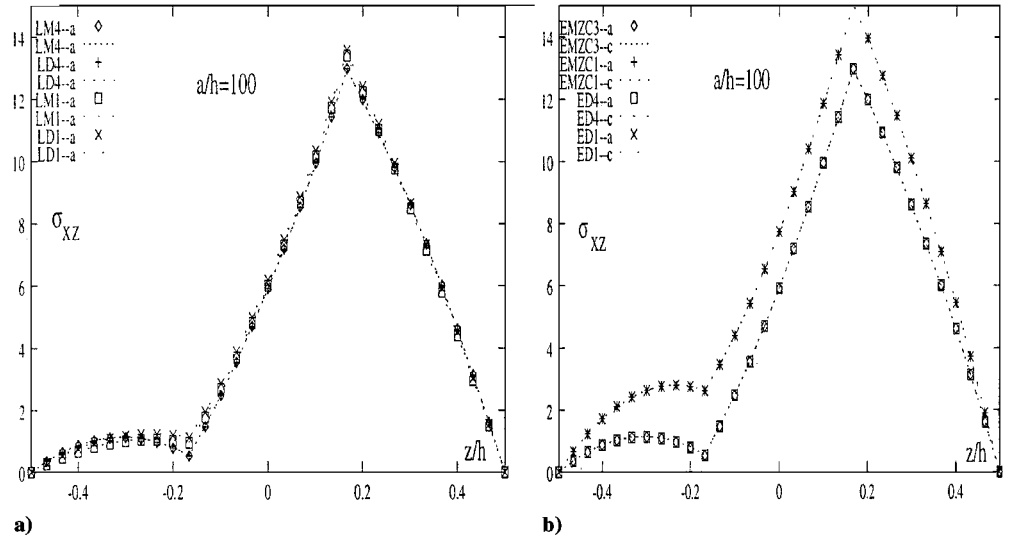

a) b)

Fig. 12 Problem 2, thin plate: a) LW and b) ESL theory.

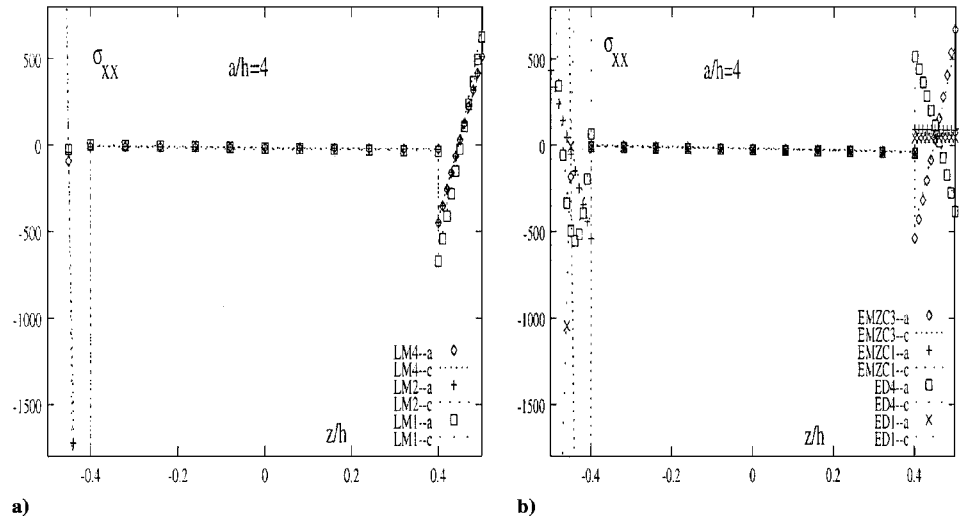

Fig. 13 Problem 3, thick plate: a) LW and b) ESL theory.

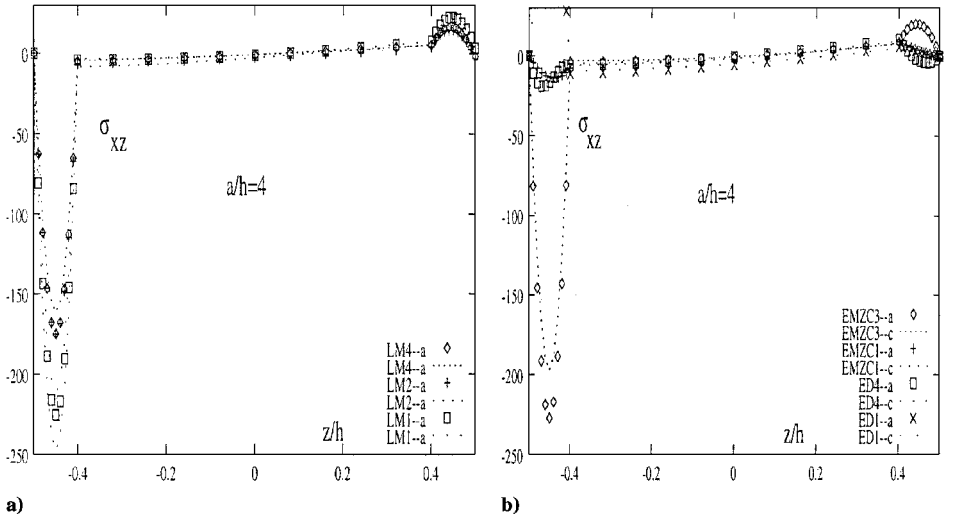

Fig. 14 Problem 3, thick plate: a) LW and b) ESL theory.

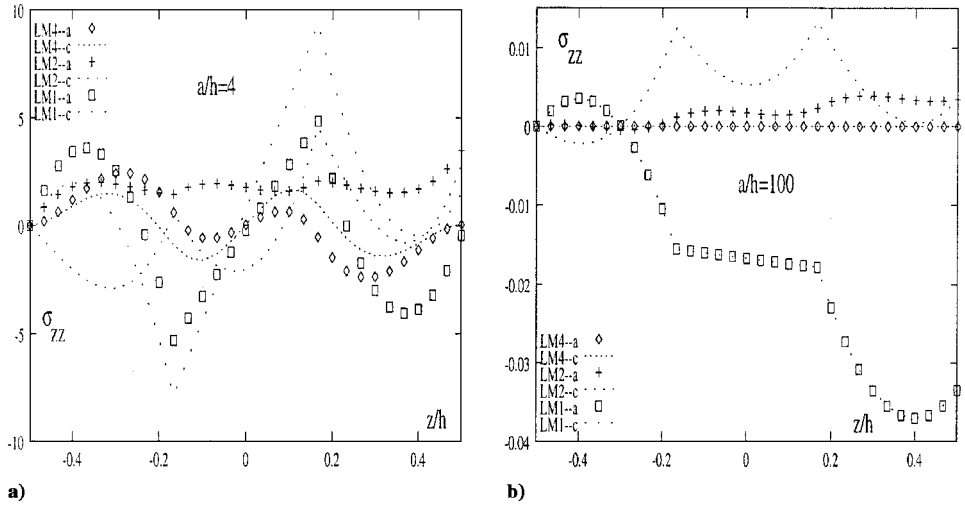

Fig. 15 Problem 4 LW theories for a) thick and b) thin plates.

Conclusions

This paper describes the investigation of the influence of the temperature profile in the thickness plate directions $T(z)$ on the response of layered, anisotropic plates. The heat conduction problem is solved, and $T_c(z)$ is calculated. The influence of temperature profile on the accuracy of plate models is then analyzed for a large variety of classical and advanced multilayered plate theories. The approximations introduced by a given plate theory are compared to those introduced by enforcing a linear temperature profile T_a. Four sample plate problems are proposed and investigated. These are related to isotropic, cross-ply laminated, and sandwich plates. The results for stresses and displacements are given for thick and thin geometries. The following main conclusions can be made:

1) The solution of the heat conduction problem has shown that thick plates show a temperature profile that can differ considerably from the linear form that is mostly assumed in the open literature.

Higher-order expansions or LW descriptions for $T_{(z)}$ should be conveniently adopted in thick geometries.

2) Calculated and assumed linear temperature profiles lead to very different plate responses.

3) Refinements of classical plate theories could result in meaningless solutions unless the effective temperature profile is employed in the calculations.

4) Because of the isotropic nature of thermal loadings, plate theories that neglect transverse normal strains lead to very inaccurate results in both thick- and thin-plates analysis. At least a parabolic expansion for transverse displacement u_z is required to capture linear thermal strains.

5) Advanced zigzag theories, which have proved to be very accurate in tracing the response of layered plates loaded with mechanical loadings, could result to be inadequate in thermomechanical problems related to thick plates.

Appendix: Explicit Forms of Arrays

The arrays in mixed Hooke's law referred to a generic fiber orientation with respect to the x axis are

$$\boldsymbol{C}^k_{pp} = \begin{bmatrix} C^k_{11} & C^k_{12} & C^k_{16} \\ C^k_{12} & C^k_{22} & C^k_{26} \\ C^k_{16} & C^k_{26} & C^k_{66} \end{bmatrix}, \qquad \boldsymbol{C}^k_{pn} = \begin{bmatrix} 0 & 0 & C^k_{13} \\ 0 & 0 & C^k_{23} \\ 0 & 0 & C^k_{36} \end{bmatrix}$$

$$\boldsymbol{C}^k_{np} = \begin{bmatrix} 0 & 0 & 0 \\ 0 & 0 & 0 \\ -C^k_{13} & -C^k_{23} & -C^k_{36} \end{bmatrix}, \qquad \boldsymbol{C}^k_{nn} = \begin{bmatrix} C^k_{55} & -C^k_{45} & 0 \\ -C^k_{45} & C^k_{44} & 0 \\ 0 & 0 & C^k_{33} \end{bmatrix}$$

where

$$C^k_{ij} = \tilde{C}^k_{ij} - \frac{\tilde{C}^k_{i3}\tilde{C}^k_{3j}}{\tilde{C}^k_{33}}, \qquad i, j = 1, 2, 6$$

$$C^k_{i3} = \frac{\tilde{C}^k_{i3}}{\tilde{C}^k_{33}}, \qquad i = 1, 2, 6$$

$$C^k_{33} = \frac{1}{\tilde{C}^k_{33}}, \qquad C^k_{44} = \frac{\tilde{C}^k_{44}}{\Delta}, \qquad C^k_{55} = \frac{\tilde{C}^k_{55}}{\Delta}$$

$$C^k_{45} = \frac{\tilde{C}^k_{45}}{\Delta}, \qquad \Delta = \tilde{C}^k_{44}\tilde{C}^k_{55} - \tilde{C}^{k^2}_{45}$$

The arrays of differential operators on Ω^k are

$$\boldsymbol{D}_p = \begin{bmatrix} \partial_x & 0 & 0 \\ 0 & \partial_y & 0 \\ \partial_y & \partial_x & 0 \end{bmatrix}, \qquad \boldsymbol{D}_n = \begin{bmatrix} \partial_z & 0 & \partial_x \\ 0 & \partial_z & \partial_y \\ 0 & 0 & \partial_z \end{bmatrix}$$

$$\boldsymbol{D}_{n\Omega} = \begin{bmatrix} 0 & 0 & \partial_x \\ 0 & 0 & \partial_y \\ 0 & 0 & 0 \end{bmatrix}, \qquad \boldsymbol{D}_{nz} = \begin{bmatrix} \partial_z & 0 & 0 \\ 0 & \partial_z & 0 \\ 0 & 0 & \partial_z \end{bmatrix}$$

Further arrays introduced at Eq. (34) are

$$\boldsymbol{I} = \begin{bmatrix} 1 & 0 & 0 \\ 0 & 1 & 0 \\ 0 & 0 & 1 \end{bmatrix}, \qquad \boldsymbol{I}_p = \begin{bmatrix} 1 & 0 & 0 \\ 0 & 1 & 0 \\ 1 & 1 & 0 \end{bmatrix}, \qquad \boldsymbol{I}_{n\Omega} = \begin{bmatrix} 0 & 0 & 1 \\ 0 & 0 & 1 \\ 0 & 0 & 0 \end{bmatrix}$$

References

[1]Thornton, E. A., *Thermal Structures for Aerospace Applications*, AIAA Education Series, AIAA, Reston, VA, 1996.

[2]Murakami, H., "Assessment of Plate Theories for Treating the Thermomechanical Response of Layered Plates," *Composites Engineering*, Vol. 3, No. 2, 1993, pp. 137–149.

[3]Creschik, G., Palisoc, A., Cassapakis, C., Veal, G., Mikulas, M. M., "Sensitivity Study of Precision Pressurized Membrane Reflector Deformations," *AIAA Journal*, Vol. 38, 2000, pp. 308–314.

[4]Zhou, X., Chattopadhyay, A., and Gu, H., "Dynamic Responses of Smart Composites Using a Coupled Thermo–Piezoelectric–Mechanical Model," *AIAA Journal*, Vol. 38, No. 10, 2000, pp. 1939–1948.

[5]Srinivas, S., and Rao, A. K., "A Note on Flexure of Thick Rectangular Plates and Laminates with Variation of Temperature Across the Thickness," *Bull. Acad. Pol. Sci. Ser. Sci. Tech.*, Vol. 20, 1972, pp. 229–234.

[6]Bapu Rao, M. N., "3D Analysis of Thermally Loaded Thick Plates," *Nuclear Engineering and Design*, Vol. 55, 1979, pp. 353–361.

[7]Tungikar, V. B., and Rao, K. M., "Three Dimensional Exact Solution of Thermal Stresses in Rectangular Composite Laminates, *Composite Structures*, 1994, Vol. 27, pp. 419–427.

[8]Bhaskar, K., Varadan, T. K., and Ali, J. S. M., "Thermoelastic Solution for Orthotropic and Anisotropic Composites Laminates," *Composites*, Pt. B, Vol. 27B, 1996, pp. 415–420.

[9]Carrera, E., "A Class of Two Dimensional Theories for Multilayered Plates Analysis," *Atti Accademia delle Scienze di Torino, Mem. Sci. Fis.*, 19-20, Turin, Italy, 1995, pp. 49–87.

[10]Tauchert, T. R., "Thermally Induced Flexure, Buckling and Vibration of Plates," *Applied Mechanics Reviews*, Vol. 44, No. 8, 1991, pp. 347–360.

[11]Noor, A. K., and Burton, W. S., "Computational Models for High–Temperature Multilayered Composite Plates and Shells," *Applied Mechanics Reviews*, Vol. 45, No. 10, 1992, pp. 419–446.

[12]Argyris, J., and Tenek, L., "Recent Advances in Computational Thermostructural Analysis of Composite Plates and Shells with Strong Nonlinearities," *Applied Mechanics Reviews*, Vol. 50, No. 5, 1997, pp. 285–306.

[13]Reddy, J. N., *Mechanics of Laminated Composite Plates, Theory and Analysis*, CRC Press, Boca Raton, FL, 1997.

[14]Carrera, E., "An Assessment of Mixed and Classical Theories for the Thermal Stress Analysis of Orthotropic Plate Multilayerd Plates," *Journal of Thermal Stress*, Vol. 23, 2000, pp. 797–831.

[15]Bhaskar, K., and Varadan, T. K., "A New Theory for Accurate Thermal/Mechanical Flexural Analysis of Symmetric Laminated Plates," *Composite Structures*, Vol. 45, 1999, pp. 227–232.

[16]Gu, H., Chattopadhyay, A., Li, J., and Zhou, C., "A Higher Order Temperature Theory for Coupled Thermo-Piezoelectric-Mechanical Modeling of Smart Structures," *International Journal of Solids and Structures*, Vol. 37, 2002, pp. 6479–6497.

[17]Carrera, E., "Evaluation of Layerwise Mixed Theories for Laminated Plates Analysis," *AIAA Journal*, Vol. 36, No. 5, 1998, pp. 830–839.

[18]Carrera, E., "Layer-Wise Mixed Models for Accurate Vibration Analysis of Multilayered Plates," *Journal of Applied Mechanics*, Vol. 65, 1998, pp. 820–829.

[19]Carrera, E., "A Study of Transverse Normal Stress Effects on Vibration of Multilayered Plates and Shells," *Journal of Sound and Vibration*, Vol. 225, 1999, pp. 803–829.

[20]Carrera, E., "Single- vs Multilayers Plate Modelings on the Basis of Reissner's Mixed Theorem," *AIAA Journal*, Vol. 38, No. 2, 2000, pp. 342–352.

[21]Carrera, E., "Developments, Ideas and Evaluations Based upon the Reissner's Mixed Variational Theorem in the Modeling of Multilayered Plates and Shells," *Applied Mechanics Reviews*, Vol. 54, 2001, pp. 301–329.

[22]Kheider, A. A., and Reddy, J. N., "Thermal Stress and Deflections of Cross-Ply Laminated Plates Using Refined Theories," *Journal of Thermal Stress*, Vol. 12, pp. 321–332.

[23]Cho, K. N., Bert, C. W., and Striz, A. G., "Thermal Stress Analysis of Laminate Using Higher Order Individual-Layer Theory," *Journal of Thermal Stress*, Vol. 12, 1989, pp. 321–332.

[24]Murakami, H., "Laminated Composite Plate Theory with Improved In-plane Response," *Journal of Applied Mechanics*, Vol. 53, 1986, pp. 661–666.

[25]Reissner, E., "On a Certain Mixed Variational Theory and a Proposed Applications," *International Journal of Numerical Methods in Engineering*, Vol. 20, 1984, pp. 1366–1368.

[26]Reissner, E., "On a Mixed Variational Theorem and on a Shear Deformable Plate Theory," *International Journal of Numerical Methods in Engineering*, Vol. 23, 1986, pp. 193–198.

[27]Jones, R. M., *Mechanics of Composite Materials*, McGraw–Hill, New York, 1975.

A. Chattopadhyay
Associate Editor